Slag-Based Nitrogen Removal From Third-Generation Advanced High-Strength Steel

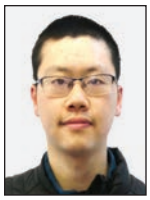


Authors

Panwen Su (left)
Research Associate, Carnegie Mellon University, Pittsburgh, Pa., USA

P. Chris Pistorius (right)
POSCO Professor of Materials Science and Engineering; Co-Director, Center for Iron and Steelmaking Research, Carnegie Mellon University, Pittsburgh, Pa., USA

Nitrogen removal by Al_2O_3-CaO-MgO-SiO_2 slags (<15 wt.% SiO_2) from third-generation advanced high-strength steel (at 1,873 K, 1 atm) was studied with FactSage calculations and laboratory slag-steel reactions. The expected nitrogen distribution coefficient between slag and steel is in the range of 20–60. Nitrogen removal to these low-SiO_2 slags occurs despite a relatively low nitride capacity, thanks to the highly reducing conditions bestowed by the high concentrations of dissolved Al, Si or both of these.

This paper is the recipient of the 2023 AIST Ladle & Secondary Refining Best Paper Award. To learn more about AIST awards, visit AIST.org.

Third-generation advanced high-strength steel (AHSS) (Fe-Mn-Al-Si-C-based) for automobile manufacturing must meet high standards of both strength and ductility (> 1 GPa yield strength plus ~30% elongation).[1] To obtain such excellent mechanical properties, impurity removal by ladle treatment is needed. Table 1 shows typical reductions of the main impurities (S, O and N) after ladle treatment.[2]

Dissolved oxygen and sulfur are readily removed during ladle treatment — by adding deoxidizers, and treatment with a basic slag. However, little removal of dissolved nitrogen is possible, because of the high solubility of nitrogen in these manganese-rich steels and unfavorable kinetics.[3]

Slag-based nitrogen removal is the primary focus of this work instead. Nitrogen absorption by the slag is feasible because of the highly reducing conditions that result from the relatively high concentration of dissolved aluminum (around 1% by mass, much higher than in low-carbon aluminum-killed steel). Nitrogen removal involves reduction of dissolved nitrogen to nitride ions (N^{3-}), which dissolve in the slag.

Laboratory experiments (not presented here) have demonstrated that slag-based nitrogen removal is possible. Here, the nitrogen removability with ladle slag (Al_2O_3-CaO-MgO-SiO_2 system, SiO_2 ≤5%, CaO 40–60%, MgO 0–10%) is evaluated with FactSage calculations. FactSage[4] was used to predict the equilibrium nitrogen solubility in ladle slag and to perform kinetic simulations of slag-steel reactions.

Table 1

Typical Values of Impurity Levels in Liquid Steel After Ladle Refining[2]

Impurity	Concentration	
	After BOF/EAF tap (ppm)	After ladle refining (ppm)
S	70–350	30–50
O	650–700	<5
N	~50	similar

Simulation Conditions

FactSage Calculations: Single-Point Equilibrium — The equilibrium nitrogen solubility in slag can be expressed with the nitrogen distribution coefficient (L_N) and the nitride capacity ($C_{N^{3-}}$):[5]

$$C_{N^{3-}} = (\text{N\% by mass in slag}) \times (p_{O_2})^{0.75} / (p_{N_2})^{0.5} \text{ (for pressures in atm)}$$

$$L_N = (\text{N \% by mass in slag})/[\text{N \% by mass in steel}]$$

Table 2

Calculated Steel-Slag Equilibrium at 1,600°C, for Slag Double Saturated With Lime and Periclase

Slag	CaO	Al_2O_3	MgO	SiO_2	N	Steel	Mn	Al	Si	C	Mg	N	p_{N_2} (atm)	p_{O2} (atm)	LN	$C_{N^{3-}}$
Mass %	51.8	41.7	6.9	0.1	0.8	Mass %	2.4000	0.6800	0.6800	0.2000	0.0053	0.0110	5.6×10^{-2}	3.6×10^{-18}	76	2.8×10^{-13}

Table 3

Initial Steel Composition for Steel-Slag Reactions (mass percentages)

Fe	Al	C	Mn	N	O	S	Si
Balance	0.830	0.200	2.800	0.005–0.015	0.010	~0.001	0.451

For equilibrium calculations, the FactSage solution phases were FTmisc_FeLQ for liquid steel (suppressing the Ca*O associate), FTOxCN-Slag for liquid slag, FToxidMeO_A for lime (CaO-based solid solution) and periclase (MgO-based solid solution), and FactPS for the gas phase. As an example, Table 2 shows the calculated equilibrium of steel with slag that is doubly saturated with lime and periclase, at 1,600°C. The calculated nitrogen distribution coefficient is large — thanks to the low oxygen activity — despite the relatively small nitride capacity. With a distribution coefficient of 76, and a typical slag-to-steel mass ratio of 0.01 for ladle refining, the fraction of the total nitrogen that would be removed to the slag is given by $1 - 1/(1 + L_N W_{slag}/W_{steel}) = 0.43$ (where W_{slag} and W_{steel} are the steel and slag masses). That is, more than 40% of the nitrogen could be removed by slag-steel reaction during ladle refining. Lower temperatures would improve the equilibrium nitrogen removal somewhat. For example, at 1,550°C the equilibrium nitrogen distribution coefficient for these conditions is predicted to be 98.

Table 2 also indicates the very low equilibrium SiO_2 concentration in the slag: Al in the steel tends to reduce SiO_2 from the slag.

Kinetic Simulation: FactSage Macro Calculations — The kinetics of slag-based nitrogen removal from liquid steel was modeled using FactSage macro calculations. The assumption is that the reaction rate is limited by mass transfer in the steel and slag, with local equilibrium reached at the steel-slag interface.[6]

Both laboratory (crucible) and industrial (ladle) conditions were simulated. The main differences were the much larger slag: steel mass ratio for laboratory experiments (to ensure that the steel is covered by slag), and the smaller mass transfer coefficient under laboratory conditions (though giving a similar time constant for steel-slag reactions), because of the much smaller depth of steel (inner diameter = 56 mm, with the depth of steel ~3 cm in the laboratory crucible).

The initial steel composition was as shown in Table 3. The ladle parameters for the simulation were as listed in Table 4. The solution models and assumed mass

Table 4

Ladle Parameters for FactSage Simulations

Ar flowrate, V_{Ar} (Nm^3/s)	0.01
Temperature of liquid steel, T (K)	1,873
Mass of liquid steel, W_{steel} (t)	180
Ladle diameter, d_{ladle} (m)	2.6
Mass transfer coefficient[9]	$m = 8.33 \times 10^{-7}\ (E/A)$ (m/s)
	E = stirring power of Ar bubbles (W)
	A = projected steel-slag interfacial area (m^2)
	$E = 371 V_{Ar} T \left[-\frac{298}{T} + \ln\left(\frac{p_{bottom}}{p_{top}} \right) \right]$
	V_{Ar} = Ar flowrate (Nm^3/s)
	p_{top} = pressure at the steel top (Pa)
	p_{bottom} = pressure at the steel bottom (Pa)
	$p_{bottom} = p_{top} + (\rho_{steel} g h_{steel})$
	ρ_{steel} = liquid steel density (kg/m^3)
	g = 9.81 m/s^2 (gravitational acceleration)
	h_{steel} = depth of liquid steel bath (m)

Table 5

Solution Models and Parameters Used for FactSage Macro Simulations

Phase	Solution model	
Liquid steel	FTmisc FeLQ	
Slag	FTOxCN-slag	
Solid oxides	FToxid-A-monoxide; FToxid-B-spinel; FToxid-corundum; FToxid-a-$(Ca,Sr)_2SiO_4$	
Simulation parameters	Slag density, ρ_{slag}	2,500 kg/m^3
	Steel density, ρ_{steel}	7,000 kg/m^3
	Slag-to-steel mass ratio	1:4 (crucible); 1:100 (ladle)
	Steel mass transfer coefficient m_{steel}	3.1×10^{-5} m/s (crucible)[8] 7.4×10^{-3} m/s (ladle)[9]
	Slag mass transfer coefficient m_{slag}	0.1 m_{steel}

Table 6

Initial Slag Compositions for Crucible and Ladle Simulations

$\%Al_2O_3$	%CaO	%MgO	$\%SiO_2$
42.3	51.2	6.5	0.0
36.7	53.5	5.6	4.0
35.0	54.0	6.0	5.0

Figure 1

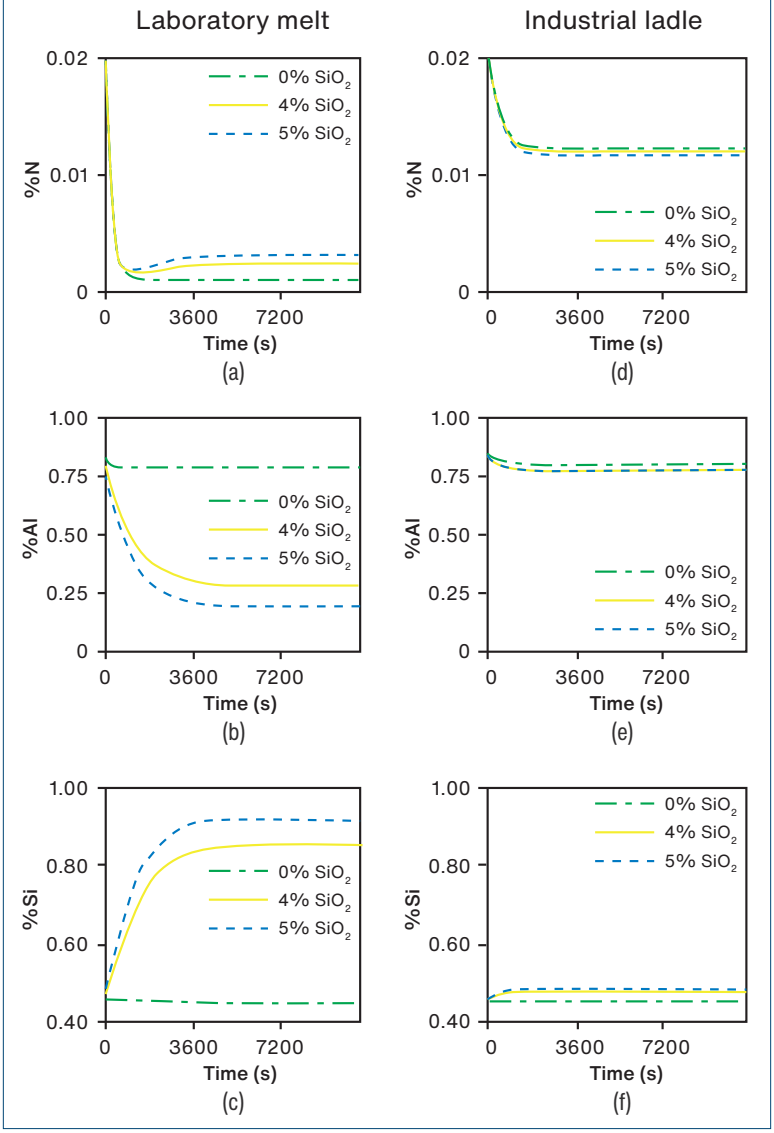

Calculated change in the concentrations of nitrogen, aluminum and silicon in steel during steel-slag reaction for a laboratory melt (a–c) and in an industrial ladle (d–f).

transfer coefficients are given in Table 5. To avoid unrealistic Ca transfer to the steel, the Ca*O associate in the steel was suppressed.

Three different initial slag compositions were chosen for simulation, as listed in Table 6. Due to the possible emulsification of steel liquid droplet into slag in crucibles, a factor called dynamic interfacial factor, defined as the ratio (A/A_0), is employed. In this ratio, A = the actual slag-steel interfacial area due to emulsification during the ladle refinement, A_0 = geometrical cross-section area of the crucible/ladle for the simulation. This starts from the time-averaged value of A/A_0 given by Spooner et al. (A/A_0 ~5).[7]

Results and Discussion

The simulated time dependence of the steel composition for both laboratory and industrial melts is shown in Fig. 1. Because of the much larger relative slag volume for the laboratory melt, the change in steel composition is much larger (Fig. 1a–1c) than for the industrial melt (Fig. 1d–1f). The large decrease in aluminum concentration, and the associated silicon pickup reflect the low equilibrium concentration of SiO_2 in the slag (Table 2): The Al-Al_2O_3 reaction controls the (low) oxygen activity for this steel-slag system; dissolved aluminum would reduce SiO_2 from the slag, causing silicon pickup by the steel. Reduction of silica by a high concentration of aluminum is known to promote emulsification of the slag.[10] Such emulsification would increase the steel-slag interfacial area, further enhancing the rate of steel-slag reactions — including nitrogen removal.

Reduction of MgO from the slag is also predicted to occur, increasing the concentration of dissolved magnesium in the steel (Table 2). The relatively high concentration of dissolved magnesium would increase the rate of transformation of alumina inclusions to spinels and periclase (MgO). This transformation has been observed experimentally for AHSS in contact with ladle slag.[11]

In line with the equilibrium calculations, approximately 40% of the dissolved nitrogen is predicted to be removed during ladle processing within approximately one hour. Faster nitrogen removal would be obtained with stronger stirring, for example in a vacuum tank degasser, or a higher argon flowrate, or both of these.

The extent of nitrogen removal under laboratory conditions is predicted to be much larger (in line with experimental results obtained to date). Some reversion of nitrogen is predicted to occur if the slag initially contains silica. The reversion occurs because of consumption of aluminum by the silica reduction reaction, causing conditions to be somewhat less reducing, and decreasing the driving force for nitrogen removal to the slag.

Conclusions

The following conclusions could be drawn from the work described in this project:

1. The Al-Al_2O_3 reaction controls the oxygen activity for liquid AHSS in contact with ladle slag.
2. Reduction of SiO_2 and MgO from the slag (increasing the concentrations of dissolved Si and Mg) is predicted to occur by steel-slag reaction during ladle processing.
3. For the conditions assumed here (steel containing approximately 0.7% dissolved Al, in contact with ladle slag saturated with both lime and periclase, at 1,600°C), more than 40% nitrogen removal from liquid steel is predicted to be possible, even with a relatively small slag volume of 10 kg slag per metric ton steel.
4. The equilibrium nitrogen concentration in the steel is predicted to be slightly lower at a lower ladle refining temperature.

Acknowledgments

The authors are grateful for the assistance provided by lab co-workers including Stephano Piva, Drew Huck, Tommy Britt and Peter Wilkerson, and staff in the Department of Materials Science and Engineering at Carnegie Mellon University. Support by the members of the Center for Iron and Steelmaking Research is gratefully acknowledged.

References

1. S. Keeler, M. Kimchi and P.J. Mooney, Advanced High-Strength Steels Application Guidelines Version 6.0, WorldAutoSteel, 2017.
2. B.A. Webler, The Making, Shaping and Treating of Steel: 101, Pittsburgh, Pa., USA, 2021.
3. D. Tang and P.C. Pistorius, "Kinetics of Nitrogen Removal From Liquid Third Generation Advanced High-Strength Steel by Tank Degassing," *Metallurgical and Materials Transactions B,* Vol. 53, 2022, 1383–1395.
4. C.W. Bale, E. Bélisle, P. Chartrand, S.A. Decterov, G. Eriksson, A.E. Gheribi, K. Hack, I.H. Jung, Y.B. Kang, J. Melançon, A.D. Pelton, S. Petersen, C. Robelin. J. Sangster, P. Spencer and M-A. Van Ende, "FactSage Thermochemical Software and Databases – 2010–2016," *Calphad,* Vol. 54, September 2016, pp. 35–53.
5. I. Jung, "Thermodynamic Modeling of Gas Solubility in Molten Slags (I) Carbon and Nitrogen," *ISIJ International,* Vol. 46, No. 11, 2006, pp. 1577–1586.
6. M. Van Ende, Y. Kim, M. Cho, J. Choi and I. Jung, "A Kinetic Model for the Ruhrstahl Heraeus (RH) Degassing Process," *Metallurgical and Materials Transactions B,* Vol. 42, No. 3, June 2011, pp. 477–489.
7. A.D. Assis, J. Warnett, S. Spooner, R. Fruehan, M. Williams and S. Sridhar, "Spontaneous Emulsification of a Metal Drop Immersed in Slag Due to Dephosphorization: Surface Area Quantification," *Metallurgical and Materials Transactions B,* Vol. 46, No. 2, April 2015, pp. 568–576.
8. S. Piva and P. Pistorius, "Ferrosilicon-Based Calcium Treatment of Aluminum-Killed and Silicomanganese-Killed Steels," *Metallurgical and Materials Transactions B,* Vol. 52, No. 1, February 2021, pp. 6–16.
9. A. Ishii, M. Tate, T. Ebisawa, and K. Kawakami, "The Ladle Refining Process for Alloyed Oil Country Tubular Goods Steels at Nippon Kokan KK," *Iron and Steelmaker,* July 1983, pp. 35–42.
10. M. Olette, "Interfacial Phenomena and Mass Transfer in Extractive Metallurgy," *Steel Research,* Vol. 59, No. 6, 1988, pp. 246–256.
11. D. Tang and P.C. Pistorius, "Inclusion Evolution in a Liquid Third-Generation Advanced High-Strength Steel in Contact With Double-Saturated Slag," *Metallurgical and Materials Transactions B,* Vol. 52, 2021, pp. 580–585. ✦

This paper was presented at AISTech 2022 – The Iron & Steel Technology Conference and Exposition, Pittsburgh, Pa., USA, and published in the AISTech 2022 Conference Proceedings.